

Tapered laminate designs for new Non-Crimp Fabric architectures.

Christopher Bronn York^{1,2} and Sérgio Frascino Müller de Almeida

Department of Mechatronics and Mechanical Systems Engineering, University of São Paulo, Av. Professor Mello Moraes, 2231, São Paulo, SP, 05508-030, Brazil.

Abstract: Non-Crimp Fabric (NCF) materials are now available in a range of areal weights and layer architectures, including 0/45, 0/-45, 45/-45 and 0/90, which correspond to the standard ply orientations employed in traditional UD material lay-ups. The benefit of NCF material is generally associated with increased deposition rate, but this advantage may be offset by reduced design freedoms when a specific form of mechanical coupling behaviour is required, layer terminations must be introduced and/or thermal warping distortion eliminated.

This article investigates the extent to which new NCF architectures can be tailored to achieve warp free tapered laminates with mechanical *Extension-Shearing Bending-Twisting* couplings, by single axis (longitudinal) deposition of all ply angles; thus avoiding ply discontinuities that may be introduced in large component manufacture.

Lamination parameter design spaces are used to demonstrate the extent of the feasible solutions both before and after applying a laminate tapering scheme.

Keywords: A. Laminate Taper; B. Extension-Shearing Coupling; C. Bending-Twisting Coupling; D. Non-Crimp Fabrics.

¹Permanent address: Aerospace Sciences, School of Engineering, University of Glasgow, University Avenue, G12 8QQ, Glasgow, Scotland.

²Corresponding author: Tel: +44 (0)141 3304345, E-mail address: Christopher.York@Glasgow.ac.uk

1. Introduction

Design issues associated with tapered composite laminates have been comprehensively reviewed in a number of articles [1,2]. These reviews reveal an extensive literature, focussing primarily on delamination initiation and propagation in the region of ply terminations, but also reveal that little attention has been given to the extent to which plies may be dropped without introducing thermal warping distortion and associated changes in mechanical coupling characteristics. Indeed, current tapering schemes tend to consider only short ramps or pad-ups, and few [3] consider thermal warping and the associated locked in stresses. By contrast, tapering schemes for continuous wing or fuselage panel construction, in which only single ply terminations may be necessary between adjacent ribs or ring stiffeners, to satisfy strength and/or buckling constraints, are currently restricted to balanced and symmetric laminate designs. Hence, with few exceptions [4], such designs generally require a minimum of 4 ply terminations to avoid introducing thermal warping distortions; their inherent mechanical *Bending-Twisting* coupling characteristics can also lead to significant reductions in the compression buckling strength [5].

New joint requirements for aero-elastic tailoring and more efficient manufacturing of composite wing or winglet construction requires a more considered tapering scheme, which has resulted in the recent development of bi-angle non-crimp fabrics (NCF) architectures, consisting of two plies of UD material, one at 0° and the other at either a shallow angle, $\theta \geq 20^\circ$, or the standard 45° angle, stitched together. The repeating bi-angle $[\theta/0]_T$ NCF concept [6] has the potential to reduce wet lay-up times by half, in comparison to traditional UD tape. In what follows, a layer (of NCF material) contains 2 plies (of UD material). Ply terminations can also be applied to any layer without

changing the *Extension-Shearing* and *Bending-Twisting* dominant mechanical coupling, necessary for aero-elastic tailoring of wing-box structures. However, thermal warping distortions are eliminated only when the number of repeats (r) remain large.

Recent research has however demonstrated that tailored Non-Crimp Fabric (NCF) designs, based on 0/45 and 0/-45 architectures, can produce fully uncoupled laminates or laminates with *Extension-Shearing* and/or *Bending-Twisting* coupling, and that all have immunity to thermal warping distortion [7]. The extent to which tapered laminate designs can be achieved, without introducing unwanted thermo-mechanical coupling, was also investigated through a layer termination algorithm to introduce single-layer [8] or, where necessary, multiple-layer terminations [4,7]. This research followed related studies on laminate design for uni-directional (UD) fibre architectures for fully uncoupled laminates [9], and those with *Extension-Shearing* [10] and/or *Bending-Twisting* coupling [11,12].

The results presented in this article investigate these four laminate classes constructed from the new NCF architectures, see Fig. A1 of the electronic annex. All are designed for immunity to thermal warping distortions by virtue of the fact that their coupling stiffness properties are null ($\mathbf{B} = \mathbf{0}$); as would be expected from symmetric laminate configurations. Two classes contain balanced angle plies, leading to uncoupled extensional stiffness properties. The so called *Simple* laminate is also uncoupled in bending, whilst the laminate class in the second column possesses *Bending-Twisting* or *B-T* coupling. The two other laminate classes possess unbalanced angle plies, leading to *Extension-Shearing* or *E-S* coupling properties. One is uncoupled in bending and other has both *Extension-Shearing* and *Bending-Twisting* or *E-S;B-T* coupling, as would arise from unbalanced and symmetric laminates.

The main purpose of the investigation is to determine the extent to which new architectures, based on 0/45, 0/-45, 45/-45 and 0/90 NCF, can be tailored to achieve warp free tapered laminates with specific mechanical properties, but without the need for off axis alignment, and the ply discontinuities that this may cause. Off axis alignment of a 0/-45 layer, to produce a 90/45 layer, results in fibre discontinuity if the length of the part exceeds the width of the roll (commercially available widths are 1.27m, 2.54m or 3.30m).

The remainder of this article is arranged as follows. Section 2 provides a summary of mechanical coupling properties for the warp free laminate classes. Section 3 provides details of the development of the stacking sequences, the non-dimensional parameters, which may be used to calculate stiffness properties for any fibre/resin system, and the relationship between non-dimensional parameters and lamination parameters. A layer termination algorithm is described in Section 4, which is then applied to *Extension-Shearing Bending-Twisting* coupled laminates to develop tapered designs with consistent mechanical coupling properties throughout. Results are presented in Section 5, including design space comparisons and tapered designs. Finally, conclusions are drawn in Section 6.

2. Summary of Mechanical Coupling properties for warp free design

Simple, *Extension-Shearing* and/or *Bending-Twisting* coupled laminates all share the common feature that couplings between in-plane and out-of-plane responses, hence thermal warping distortions, are eliminated by virtue of the fact that $B_{ij} = 0$ in Eq. (1). However, coupling between *Extension* and *Shearing* is present when $A_{xs} = A_{ys} \neq 0$, and between *Bending* and *Twisting* when $D_{xs} = D_{ys} \neq 0$.

$$\begin{aligned}
\begin{Bmatrix} N_x \\ N_y \\ N_s \end{Bmatrix} &= \begin{bmatrix} A_{xx} & A_{xy} & A_{xs} \\ A_{xy} & A_{yy} & A_{ys} \\ A_{xs} & A_{ys} & A_{ss} \end{bmatrix} \begin{Bmatrix} \varepsilon_x \\ \varepsilon_y \\ \gamma_s \end{Bmatrix} + \begin{bmatrix} B_{xx} & B_{xy} & B_{xs} \\ B_{xy} & B_{yy} & B_{ys} \\ B_{xs} & B_{ys} & B_{ss} \end{bmatrix} \begin{Bmatrix} \kappa_x \\ \kappa_y \\ \kappa_s \end{Bmatrix} \\
\begin{Bmatrix} M_x \\ M_y \\ M_s \end{Bmatrix} &= \begin{bmatrix} B_{xx} & B_{xy} & B_{xs} \\ B_{xy} & B_{yy} & B_{ys} \\ B_{xs} & B_{ys} & B_{ss} \end{bmatrix} \begin{Bmatrix} \varepsilon_x \\ \varepsilon_y \\ \gamma_s \end{Bmatrix} + \begin{bmatrix} D_{xx} & D_{xy} & D_{xs} \\ D_{xy} & D_{yy} & D_{ys} \\ D_{xs} & D_{ys} & D_{ss} \end{bmatrix} \begin{Bmatrix} \kappa_x \\ \kappa_y \\ \kappa_s \end{Bmatrix}
\end{aligned} \tag{1}$$

Whilst Eq. (1) describes the well-known **ABD** relation from classical laminate plate theory, it is more often expressed using compact notation:

$$\begin{Bmatrix} \mathbf{N} \\ \mathbf{M} \end{Bmatrix} = \begin{bmatrix} \mathbf{A} & \mathbf{B} \\ \mathbf{B} & \mathbf{D} \end{bmatrix} \begin{Bmatrix} \boldsymbol{\varepsilon} \\ \boldsymbol{\kappa} \end{Bmatrix} \tag{2}$$

The coupling behaviour, which is dependent on the form of the elements in each of the extensional **[A]**, coupling **[B]** and bending **[D]** stiffness matrices, is now described by an extended subscript notation, defined previously by the Engineering Sciences Data Unit, or ESDU [13] and subsequently augmented for the purposes of this series of articles. Hence, laminates with coupling between *Extension* and *Shearing*, and *Bending* and *Twisting*, are referred to by the designation **A_FB₀D_F**, signifying that the elements of the extensional stiffness matrix **[A]** are finite, i.e.:

$$\begin{bmatrix} A_{xx} & A_{xy} & A_{xs} \\ A_{xy} & A_{yy} & A_{ys} \\ A_{xs} & A_{ys} & A_{ss} \end{bmatrix} \tag{3}$$

the coupling matrix **[B]** is null, whilst all elements of the bending stiffness matrix **[D]** are finite, i.e.:

$$\begin{bmatrix} D_{xx} & D_{xy} & D_{xs} \\ D_{xy} & D_{yy} & D_{ys} \\ D_{xs} & D_{ys} & D_{ss} \end{bmatrix} \tag{4}$$

Note that the term *fully uncoupled orthotropic* laminate is synonymous with *specially orthotropic* or *Simple* laminate. Such laminates possess none of the coupling characteristics described above and are represented by the designation $\mathbf{A}_S\mathbf{B}_0\mathbf{D}_S$, since the elements of the extensional and bending stiffness matrices are *Simple* or specially orthotropic in nature, e.g. the bending stiffness matrix $[\mathbf{D}]$ contains $D_{xs} = D_{ys} = 0$.

Extensionally Isotropic laminates, with the designation $\mathbf{A}_I\mathbf{B}_0\mathbf{D}_S$ and Fully Isotropic laminates, with the designation $\mathbf{A}_I\mathbf{B}_0\mathbf{D}_I$, represent sub-sets of *Simple* laminates and are useful for benchmarking purposes. In the former case, the extensional stiffness matrix with designation \mathbf{A}_S is replaced with \mathbf{A}_I to indicate extensional isotropy, given that:

$$A_{xx} = A_{yy} \quad (5)$$

$$A_{ss} = (A_{xx} - A_{xy}) / 2 \quad (6)$$

$$A_{xs} = A_{ys} = 0 \quad (7)$$

In the latter case, the bending stiffness matrix with designation \mathbf{D}_S is replaced with \mathbf{D}_I to indicate bending isotropy, and hence full isotropy, given that, in addition to the Eqs (5) and (6):

$$D_{ij} = A_{ij}H^2 / 12 \quad (8)$$

where H is the laminate thickness.

Quasi-Homogeneous laminates possess concomitant stiffness properties, i.e. matching stiffness in extension and bending, as described by Eq. (8); these are presented elsewhere for *Simple* or uncoupled laminates with UD material [14].

3. Derivation of stacking sequence data

The theory behind the algorithm used to generate the designs presented here is given elsewhere [9,10,11,12] for each of the 4 laminate classes. Only a summary is therefore provided here, together with details on how the previous derivation for UD laminates has been modified for the purposes of laminates with new NCF architectures.

3.1 Derivation of stacking sequences

The four design freedoms associated with the stacking sequences used in standard UD laminate manufacture, with ply orientations 0, 90, 45 and -45°, were shown [7] to increase to eight using 0/45 and 0/-45 NCF: by inverting (-45/0 and 45/0), rotating (90/-45 and 90/45) or both (45/90 and -45/90). However, rotating introduces ply discontinuity in the angle plies whenever the length of a component or structure is greater than the width of the fabric being deposited.

The four design freedoms associated with the new architectures, based on 0/45, 0/-45, 45/-45 and 0/90 NCF, are also increased to eight, but involve only inversion (-45/0, 45/0, -45/45, 90/0). Underlining is used to highlight the ply pairings. Double underlining is used to highlight the ply pairings which have been inverted.

In the derivation of the database of stacking sequences, which assumes (but is not restricted to) combinations of standard fibre angle orientations, i.e. 0, 90 and/or $\pm\theta^\circ$ ($= \pm 45^\circ$), the general rule of symmetry is relaxed. Neither cross plies nor angle plies are constrained to be symmetric about the laminate mid-plane. The derivation of the NCF laminate designs involves the added restrictions that each ply, now part of a two-ply pairing that forms a single NCF layer: has identical orthotropic material properties; has identical thickness, t , and; differs only by its orientation, chosen here to represent combination of the eight commercially available pairings: 0/45, 45/0, 0/-45, -45/0, 45/-

45, -45/45, 0/90 and 90/0. This choice facilitate laminate lay-up without the need for off-axis alignment of any layer, thus avoiding ply discontinuities whenever the part length exceeds with roll width of the NCF.

For compatibility with the previously published data, similar symbols have been adopted for defining the stacking sequences, i.e., \bigcirc , \bullet , $+$ and $-$ are used in place of standard angles 0 , 90 , $+45$ and -45° , assumed here, noting that cross plies can be arbitrarily switched within a given stacking sequence, and angle plies are commercially available within the range $20^\circ \leq \theta \leq 45^\circ$, and may be assigned to a given stacking sequence without changing the mechanical coupling behaviour.

To avoid the trivial solution of a stacking sequences with cross plies only, for *Simple* laminates, all sequences have an angle-ply ($+$) on the upper surface of the laminate. As a result, the upper surface layer may be either a $\underline{+/\bigcirc}$ or $\underline{+/-}$ ply pairing, which has implications with respect to laminate tapering, given that the surface layers are assumed to be continuous throughout. By contrast the exposed ply of the lower surface layer may be an angle ply of equal ($+$) or opposite ($-$) orientation or a cross ply (\bigcirc or \bullet), which may be either 0 or 90° .

Non-dimensional parameters allow the extensional and bending stiffness properties to be readily calculated for any fibre/matrix system and angle-ply orientation and provide a compact data set alongside each laminate stacking sequence derived.

3.2 Derivation of non-dimensional parameters

The development of non-dimensional parameters, relating to the elements of the stiffness matrices in Eq. (9), involves the summations of only the geometric parts for each ply orientation:

$$\begin{aligned}
A_{ij} &= \sum Q'_{ij} (z_k - z_{k-1}) \\
B_{ij} &= \sum Q'_{ij} (z_k^2 - z_{k-1}^2) / 2 \\
D_{ij} &= \sum Q'_{ij} (z_k^3 - z_{k-1}^3) / 3
\end{aligned} \tag{9}$$

whereby the summations extend over all n plies, Q'_{ij} are the transformed reduced stiffnesses and z_k represents the distance from the laminate mid-plane of the k^{th} ply interface. The interface distances z_k are expressed in terms of constant ply thickness t , which is set to unit value.

The geometric parts of the summations for $(z_k - z_{k-1})$ lead to the parameters n_+ , n_- , n_\circ and n_\bullet , representing the number of plies in each of the four ply orientations, whereas the summations for $(z_k^2 - z_{k-1}^2)$ lead to non-dimensional coupling stiffness parameters $\chi_+ = \chi_- = \chi_\circ = \chi_\bullet = 0$ for all the laminate classes presented here. The summations for $(z_k^3 - z_{k-1}^3)$ leads to non-dimensional bending stiffness parameters ζ_+ , ζ_- , ζ_\circ and ζ_\bullet , which have been factored by four, such that:

$$\zeta = (\zeta_+ + \zeta_- + \zeta_\circ + \zeta_\bullet) = n^3 = (n_+ + n_- + n_\circ + n_\bullet)^3 \tag{10}$$

These non-dimensional parameters, together with the transformed reduced stiffnesses, Q'_{ij} , for each ply orientation of constant ply thickness, t , facilitate simple calculation of the elements of the extensional and bending stiffness matrices from:

$$A_{ij} = [n_+ Q'_{ij+} + n_- Q'_{ij-} + n_\circ Q'_{ij\circ} + n_\bullet Q'_{ij\bullet}] t \tag{11}$$

$$D_{ij} = [\zeta_+ Q'_{ij+} + \zeta_- Q'_{ij-} + \zeta_\circ Q'_{ij\circ} + \zeta_\bullet Q'_{ij\bullet}] t^3 / 12 \tag{12}$$

Whilst the non-dimensional parameters n_+ , n_- , n_\circ and n_\bullet , are simply the number of plies in each fibre direction, the bending stiffness parameters, ζ_+ , ζ_- , ζ_\circ and ζ_\bullet , represent the individual contributions to the overall bending stiffness ζ .

Extension-Shearing and *Bending-Twisting* coupled laminates satisfy the following non-dimensional parameter criteria [12]:

$$n_+ \neq n_-, \zeta_+ \neq \zeta_- \quad (13)$$

whilst the conditions giving rise to *Bending-Twisting* coupled laminates [11] are:

$$n_+ = n_-, \zeta_+ \neq \zeta_- \quad (14)$$

the conditions giving rise to *Extension-Shearing* coupled laminates [10] are:

$$n_+ \neq n_-, \zeta_+ = \zeta_- \quad (15)$$

and the conditions giving rise to *Simple* [9] laminates are:

$$n_+ = n_-, \zeta_+ = \zeta_- \quad (16)$$

3.3 Lamination parameters

Lamination parameters, originally conceived by Tsai and Hahn [16] offer an alternative set of non-dimensional expressions when ply angles are a design constraint. They were first applied to optimum design by Miki [17] and presented in graphical form by Fukunaga and Vanderplaats [18]. Optimized lamination parameters may be matched against a corresponding set of stacking sequences. Graphical representations help with this design process, since arguably the greatest challenge to the composite laminate designer, is the inverse problem of generating practical laminate configurations, which satisfy the optimized lamination parameters.

Elements of the *Extension-Shearing* coupled extensional stiffness matrix $[\mathbf{A}]$ are related to the lamination parameters [16] by:

$$[\mathbf{A}] = H \begin{bmatrix} U_E + \xi_\Delta^A U_\Delta + \xi_R^A U_R & U_E - 2U_G - \xi_R^A U_R & \xi_{\Delta c}^A U_\Delta / 2 + \xi_{Rc}^A U_R \\ U_E - 2U_G - \xi_R^A U_R & U_E - \xi_\Delta^A U_\Delta + \xi_R^A U_R & \xi_{\Delta c}^A U_\Delta / 2 - \xi_{Rc}^A U_R \\ \xi_{\Delta c}^A U_\Delta / 2 + \xi_{Rc}^A U_R & \xi_{\Delta c}^A U_\Delta / 2 - \xi_{Rc}^A U_R & U_G - \xi_R^A U_R \end{bmatrix} \quad (17)$$

and the fully populated bending stiffness matrix $[\mathbf{D}]$ by:

$$[\mathbf{D}] = \frac{H^3}{12} \begin{bmatrix} U_E + \xi_\Delta^D U_\Delta + \xi_R^D U_R & U_E - 2U_G - \xi_R^D U_R & \xi_{\Delta c}^D U_\Delta / 2 + \xi_{Rc}^D U_R \\ U_E - 2U_G - \xi_R^D U_R & U_E - \xi_\Delta^D U_\Delta + \xi_R^D U_R & \xi_{\Delta c}^D U_\Delta / 2 - \xi_{Rc}^D U_R \\ \xi_{\Delta c}^D U_\Delta / 2 + \xi_{Rc}^D U_R & \xi_{\Delta c}^D U_\Delta / 2 - \xi_{Rc}^D U_R & U_G - \xi_R^D U_R \end{bmatrix} \quad (18)$$

where laminate invariants are defined in terms of the reduced stiffnesses:

$$\begin{aligned} U_E &= (3Q_{11} + 3Q_{22} + 2Q_{12} + 4Q_{66}) / 8 \\ U_G &= (Q_{11} + Q_{22} - 2Q_{12} + 4Q_{66}) / 8 \\ U_\Delta &= (Q_{11} - Q_{22}) / 2 \\ U_R &= (Q_{11} + Q_{22} - 2Q_{12} - 4Q_{66}) / 8 \end{aligned} \quad (19)$$

U_E and U_G are invariants in the sense that they do not vary with change of in-plane coordinates. They are associated with the equivalent isotropic properties of the laminate:

$$\begin{aligned} U_E &= E_{iso} / (1 - \nu_{iso}^2) \\ U_G &= G_{iso} \end{aligned} \quad (20)$$

where, E_{iso} , G_{iso} , and ν_{iso} , are the equivalent isotropic properties of the composite material, defined as:

$$\begin{aligned} E_{iso} &= 2(1 + \nu_{iso})G_{iso} \\ G_{iso} &= (Q_{11} + Q_{22} - 2Q_{12} + 4Q_{66}) / 8 \\ \nu_{iso} &= (Q_{11} + Q_{22} + 6Q_{12} - 4Q_{66}) / (3Q_{11} + 3Q_{22} + 2Q_{12} + 4Q_{66}) = 1 - 2U_G / U_E \end{aligned} \quad (21)$$

U_Δ is associated with the orthotropy along axes 1 and 2, i.e. parallel and perpendicular to the fibre direction, and U_R is a residual term contained in all elements of the stiffness matrices, which maintains square symmetry, as would be expected in balanced fabrics [19,20] or, in the context of the current study, the anti-symmetric angle-ply NCF design:

$[45/-45/-45/45]_A$, where $A_{11} = A_{22}$ and $D_{11} = D_{22}$, and for off-axis orientation, $A_{16} = -A_{26}$ and $D_{16} = -D_{26}$.

The above equations are identical to the original equations. Only the notation has been reformulated. The authors believe that this new notation is more intuitive, as it refers to the physical interpretation of the invariants and lamination parameters. Also, since there are only two material properties for an isotropic material, only two invariants (U_E and U_G) are used to describe the equivalent isotropic properties of the laminate. The original definition of lamination parameters uses three invariants (U_1 , U_4 and U_5) that are linearly dependent.

The ply orientation dependent lamination parameters are also related to the non-dimensional parameters, used in Eqs (11) and (12), by the following expressions:

$$\begin{aligned}
\xi_{\Delta}^A &= \left[n_{\pm} (n_{+} / n_{\pm}) \cos(2\theta_{+}) + n_{\pm} (1 - n_{+} / n_{\pm}) \cos(2\theta_{-}) \right. \\
&\quad \left. + n_o \cos(2\theta_o) + (n - n_{\pm} - n_o) \cos(2\theta_{\bullet}) \right] / n \\
\xi_R^A &= \left[n_{\pm} (n_{+} / n_{\pm}) \cos(4\theta_{+}) + n_{\pm} (1 - n_{+} / n_{\pm}) \cos(4\theta_{-}) \right. \\
&\quad \left. + n_o \cos(4\theta_o) + (n - n_{\pm} - n_o) \cos(4\theta_{\bullet}) \right] / n \\
\xi_{\Delta c}^A &= \left[n_{\pm} (n_{+} / n_{\pm}) \sin(2\theta_{+}) + n_{\pm} (1 - n_{+} / n_{\pm}) \sin(2\theta_{-}) \right. \\
&\quad \left. + n_o \sin(2\theta_o) + (n - n_{\pm} - n_o) \sin(2\theta_{\bullet}) \right] / n \\
\xi_{Rc}^A &= \left[n_{\pm} (n_{+} / n_{\pm}) \sin(4\theta_{+}) + n_{\pm} (1 - n_{+} / n_{\pm}) \sin(4\theta_{-}) \right. \\
&\quad \left. + n_o \sin(4\theta_o) + (n - n_{\pm} - n_o) \sin(4\theta_{\bullet}) \right] / n
\end{aligned} \tag{22}$$

relating to extensional stiffness, and

$$\begin{aligned}
\xi_{\Delta}^D &= \left[\zeta_{\pm} (\zeta_{+} / \zeta_{\pm}) \cos(2\theta_{+}) + \zeta_{\pm} (1 - \zeta_{+} / \zeta_{\pm}) \cos(2\theta_{-}) \right. \\
&\quad \left. + \zeta_{\circ} \cos(2\theta_{\circ}) + (\zeta - \zeta_{\pm} - \zeta_{\circ}) \cos(2\theta_{\bullet}) \right] / n^3 \\
\xi_R^D &= \left[\zeta_{\pm} (\zeta_{+} / \zeta_{\pm}) \cos(4\theta_{+}) + \zeta_{\pm} (1 - \zeta_{+} / \zeta_{\pm}) \cos(4\theta_{-}) \right. \\
&\quad \left. + \zeta_{\circ} \cos(4\theta_{\circ}) + (\zeta - \zeta_{\pm} - \zeta_{\circ}) \cos(4\theta_{\bullet}) \right] / n^3 \\
\xi_{\Delta c}^D &= \left[\zeta_{\pm} (\zeta_{+} / \zeta_{\pm}) \sin(2\theta_{+}) + \zeta_{\pm} (1 - \zeta_{+} / \zeta_{\pm}) \sin(2\theta_{-}) \right. \\
&\quad \left. + \zeta_{\circ} \sin(2\theta_{\circ}) + (\zeta - \zeta_{\pm} - \zeta_{\circ}) \sin(2\theta_{\bullet}) \right] / n^3 \\
\xi_{Rc}^D &= \left[\zeta_{\pm} (\zeta_{+} / \zeta_{\pm}) \sin(4\theta_{+}) + \zeta_{\pm} (1 - \zeta_{+} / \zeta_{\pm}) \sin(4\theta_{-}) \right. \\
&\quad \left. + \zeta_{\circ} \sin(4\theta_{\circ}) + (\zeta - \zeta_{\pm} - \zeta_{\circ}) \sin(4\theta_{\bullet}) \right] / n^3
\end{aligned} \tag{23}$$

relating to bending stiffness.

Note that $\xi_{Rc}^A = \xi_{Rc}^D = 0$ for the standard angle ply configurations chosen here, i.e., $\theta_{\pm} = \pm 45^{\circ}$. Hence the **[A]** and **[D]** matrices are separately described by three dimensional lamination parameter coordinates. These reduce to a two dimensional coordinate if either **[A]** or **[D]** are uncoupled. For the special case of material homogeneity, defined by Eq. (8), the lamination parameters $(\xi_{\Delta}^A, \xi_R^A, \xi_{\Delta c}^A) = (\xi_{\Delta}^D, \xi_R^D, \xi_{\Delta c}^D)$ through Eqs (17) and (18), hence **[A]** and **[D]** matrices are uniquely described by a single three dimensional lamination parameter coordinate.

4. Laminate Tapering Algorithm

For practical laminate design, tapering must be possible without introducing unwanted mechanical coupling behaviour or introducing undesirable warping distortions. This section therefore investigates the extent to which this restriction can be satisfied using NCF designs.

Tapered laminate designs have been developed in a two stage process: The first stage of the termination scheme involves: m layer terminations, applied in turn to specific layer combinations in every stacking sequence with n_{NCF} layers; comparison with all stacking

sequences with $n_{NCF}-m$ layers and; recording exact matches. The first (or upper surface) and last (or lower surface) plies are assumed to be continuous throughout the tapering process; this represents a practical design constraint to prevent surface ply delamination. The number of layer termination combinations changes according to the factorial relationship, $(n_{NCF} - 2)!/m!(n_{NCF} - 2 - m)!$ Repeated stacking sequences are removed from the reported data when multiple matches arise as a result of different combinations of layer terminations within a single stacking sequence. This forms a starting point for the second stage of the tapering algorithm.

The second stage of the tapering algorithm can be described as a bottom up process, and begins with stacking sequences, from the first stage, representing the minimum layer number grouping (n_{NCF}) of interest. These sequences are then algorithmically filtered through higher layer number groupings, in turn, but now only sequences compatible with the minimum layer number grouping are retained. This procedure facilitates the extension to higher layer number groupings, beyond those considered here.

Note that a two layer termination scheme applied to NCF material represents a constrained four ply termination scheme, due to ply pairing. Single layer terminations are not possible without introducing couplings that give rise to thermal warping distortions. This is due to the fact that a single \pm (or $45/-45$) layer possesses *Extension-Twisting* (and *Shearing-Bending*) coupling, a single $0/90$ layer possesses *Extension-Bending* coupling and a single $0/+$ (or $0/45$) or a $0/-$ (or $0/-45$) layer possesses all interactions between *Extension*, *Shearing*, *Bending* and *Twisting*.

5. RESULTS

The number of NCF laminate solutions for *Simple*, *Bending-Twisting* or *B-T* coupled, *Extension-Shearing* or *E-S* coupled, and *Extension-Shearing* and *Bending-Twisting* or *E-S;B-T* coupled warp-free laminate classes are reported in Table 1. Each row corresponds to a particular layer number grouping, n_{NCF} , with NCF layers and the equivalent ply number grouping, n_{UD} , with UD layers are given in parentheses, which correspond to previously derived results [8] with matching ply contiguity (≤ 2) constraint. This ply contiguity is a natural constraint, arising from the NCF architecture, which accounts for the reduced design space. The results reveal average differences of up to an order of magnitude difference between the number of possible solutions with UD and NCF layers.

The constraint of imposing an angle ply layer on the upper surface of the laminate gives rise to two distinctly separate NCF designs. The first has a \pm/\mathbf{O} upper surface layer and the second has a $\pm/-$ upper surface layer. The number of NCF laminate solutions are therefore reported separately, in Tables 2 and 3, respectively. For tapered solutions, in which a continuous outer layer is assumed, these two sets of designs are non-compatible. The architecture of the NCF upper surface layer has a marked effect of the mechanical properties, which explains the differences in the number of solutions between these two distinctly separate designs.

Plotting the lamination parameters for each stacking sequence from the definitive listing permits interrogation of the extent of resulting design space, where individual laminate stacking sequences are represented by a single point in a 3-dimensional space for both the extensional stiffness properties and the bending stiffness properties. Each point,

represents a co-ordinate, from which the extensional and bending stiffness properties may be readily determined using Eq. (17) and Eq. (18), respectively. Note that the lamination parameters reduce to a 3-dimensional space only by adoption of standard fiber orientations 0, 90, 45 and -45°. The design space is otherwise 4-dimensional and visualisation would be more problematic. The design space also simplifies to 2-dimensions in extensional stiffness for the *Simple* and *Bending-Twisting (B-T)* coupled laminates, and to 2-dimensions in bending stiffness for the *Simple* and *Extension-Shearing (E-S)* coupled laminates. Note that *Extension-Shearing* coupled laminates were found only in the highest layer (ply) number grouping investigated, i.e. n_{NCF} (n_{UD}) = 12 (24). The small number of stacking sequences for this class of laminate are listed in Table A1 of the electronic appendix, together with the lamination parameter coordinates.

Figure 2 illustrates the feasible region of laminate designs for extensional stiffness. Lamination parameter coordinates outside this triangular region cannot be manufactured with standard ply angle designs. Ply percentages are mapped onto the design space to give further insight and to help clarify the new lamination parameter definitions. The lamination parameter ξ_{Δ}^A is a measure of the relative orthotropic stiffness in the principal fibre directions, which is maximum when all fibres are aligned at 0° and minimum when all fibres are aligned at 90°. $\xi_{\Delta}^A = 0$ represents equal cross-ply percentages. By contrast, for $\xi_{\Delta}^A = 0$, the lamination parameter ξ_R^A affects all components of matrix [A]. The relative Poisson ratio of the laminate tends toward a minimum value when $\xi_R^A = 1$, i.e., a laminate with an equal number of 0° and 90° plies only, and towards a maximum value when $\xi_R^A = -1$, i.e., a laminate with an equal

number of 45° and -45° plies only. $\xi_R^A = 0$ for the equivalent isotropic laminate.

Isolines for Poisson ratio are also readily mapped onto the lamination parameter design space [17]. By contrast $\xi_{\Delta c}^A$ represents the degree of anisotropy, or *Extension-Shearing* coupling, which is maximised, i.e. $\xi_{\Delta c}^A = 1$ or -1 , when all plies are at $+45$ or -45° , respectively. *Extension-Shearing* is eliminated when the angle-ply percentages are equal, i.e. a balanced angle-ply laminate.

The ply percentages of Fig. 2 also apply to the lamination parameters for bending stiffness for the quasi-homogeneous anisotropic designs listed in Table 4. These designs satisfying the definition of quasi-homogeneity of Eq. (8) and therefore the lamination parameters for extensional stiffness, $(\xi_\Delta^A, \xi_R^A, \xi_{\Delta c}^A)$, are identical to those for bending stiffness, $(\xi_\Delta^D, \xi_R^D, \xi_{\Delta c}^D)$.

5.1 Design space comparisons.

The 2-dimensional projections for extensional and bending stiffness are illustrated in Figs A2 and A3 of the electronic annex, for *Simple* laminates with \pm/\pm and $\pm/\textcircled{0}$ upper surface layers, respectively. Similarly, 2- and 3-dimensional orthographic projections for extensional and bending stiffness are illustrated in Figs A4 and A5, for *Bending-Twisting* ($\underline{B-T}$) coupled laminates. The 3-dimensional point cloud of lamination parameters for *Extension-Shearing Bending-Twisting* or $\underline{E-S;B-T}$ coupled laminates, with a \pm/\pm upper surface layer, contained in Table 3, are illustrated as orthographic projections for extensional and bending stiffness in Figs 3 and 4, respectively. Results from Table 2, with a $\pm/\textcircled{0}$ upper surface layer, are similarly illustrated in Figs A6 and A7 of the electronic appendix. As a result of the constraint imposed by the NCF

architecture, the design space for all laminate classes is found to be substantially reduced in comparison to the equivalent UD design space, reported elsewhere [8].

5.2 Tapered designs.

For practical laminate design, tapering must be possible without introducing unwanted coupling behaviour. This section therefore presents examples of tapered laminate designs with two-layer terminations, which in the context of NCF laminates relates to a constrained 4 ply termination scheme, since each NCF layer contains one of eight pairs of ply angle combinations.

Extension-Shearing and *Bending-Twisting* or *E-S*;*B-T* coupled warp-free laminates have been chosen for the examples that follow, since this class of laminate offer the tailoring opportunities for the design of a passive-adaptive wing, which is gaining increased interest from industry. Passive-adaptive wings offer the potential for improved aerodynamic efficiencies, through coupling of bending and twisting at the wing-box level. This is achieved by the use of *Extension-Shearing* coupled laminates [10] as illustrated in the wing-box configuration of Fig. 1. This symmetric structural configuration gives rise to *Bending-Twisting* coupling deformation when unbalanced laminate skins, with *Extension-Shearing* coupling, are employed with their relative orientations aligned as shown. However, the limited number of designs for UD material, which are further reduced in the NCF designs of Tables 2 and 3, necessitates the use of *Extension-Shearing* and *Bending-Twisting* coupled designs, as previously considered by Baker [21]. The effect on buckling strength of *Bending-Twisting* coupling is discussed elsewhere [11,12,15], but detrimental effects can be eliminated to a large extent by minimizing $\xi_{\Delta c}^D$. Such designs are readily determined from the lamination parameter design spaces.

Table 5 give the number of *tapered* solutions for *Extension-Shearing* and *Bending-Twisting* or *E-S;B-T* coupled warp-free laminates, with even layer number groupings, after applying the taper algorithm, where each row corresponds to different layer number groupings, n_{NCF} . The equivalent ply number, n_{UD} , for UD layers is also indicated. The number of stacking sequences in column (2) is repeated from Table 2. Note that ply contiguity ≤ 2 is an enforced constraint by virtue of the NCF architecture, i.e., the number of adjacent plies with the same orientation can never exceed 2. Column (3) corresponds to the number of laminates from column (2) that match laminates with $n_{\text{NCF}}-2$ after applying the top-down termination scheme, i.e., the number of compatible sequences with those immediately below in the list. The number of laminates matching $n_{\text{NCF}}+2$ layer laminates are shown in parentheses, representing the number of compatible sequences with those immediately above in the list. Column (4) represents the number of laminates from column (3) matching laminates with $n_{\text{NCF}}+2$ after applying the *continuous* bottom-up termination scheme. Here the bottom-up process begins with the lowest layer number grouping. Note that whilst all 11 sequences with $n_{\text{NCF}} = 4$ are compatible with $n_{\text{NCF}} = 6$, not all sequences with $n_{\text{NCF}} = 6$ are compatible with $n_{\text{NCF}} = 8$ or those of higher layer number groupings. The design space is therefore constrained by the lowest layer number grouping of interest. The number of tapered solutions is always equal or greater than the number of laminates from which they are derived, given that there may be several layer termination options for a given stacking sequence. An example of the lamination design space for odd layer laminates with *Extension-Shearing* and *Bending-Twisting* coupling is illustrated in Figs 5 and 6, for extensional and bending stiffness, respectively. These lamination parameter design spaces demonstrate *tapered* NCF laminates from 5 to 9 layers, i.e. 10 to 18 UD plies.

All solutions arise from the single ($n_{\text{NCF}} =$) 5 layer design reported in Table 5(b) with lamination parameters $(\xi_{\Delta}^A, \xi_R^A, \xi_{\Delta c}^A) = (0.30, -0.40, 0.10)$ and $(\xi_{\Delta}^D, \xi_R^D, \xi_{\Delta c}^D) = (0.42, -0.15, 0.27)$. This single stacking sequence is compatible with 7 stacking sequences with ($n_{\text{NCF}} =$) 7 layers; there are 28 different tapered designs, depending on which layer combinations are terminated. These, in turn, are compatible with 109 stacking sequences with ($n_{\text{NCF}} =$) 9 plies, from which there are 739 tapered design combinations, and so on; this implies that a particular stacking sequence (or laminate stiffness) can be achieved by terminating appropriate layer combinations from a range of different stacking sequences. Tapered designs can be identified within the lamination parameter design spaces by strings of points originating from the single ($n_{\text{NCF}} =$) 5 layer design, through all 7 stacking sequences with ($n_{\text{NCF}} =$) 7 layers and on to compatible sequences with ($n_{\text{NCF}} =$) 9 and higher layer numbers. For any tapered design, the change in lamination parameter can be related to a change in other stiffness properties, e.g. material strength constraints can be related to the extensional lamination parameters, whilst buckling strength can be related to the bending lamination parameters, which is discussed in more detail elsewhere [15]. One set of tapered designs, originating from the single ($n_{\text{NCF}} =$) 5 layer design, and corresponding to one of ($n_{\text{NCF}} =$) 7 layer designs, is illustrated in Figs 5 and 6. The corresponding stacking sequences are listed in Table A2 of the electronic annex; together with an alternative design.

6. Conclusions

This article has demonstrated that new Non-Crimp Fabric (NCF) architectures can be tailored to achieve warp free laminates with either uncoupled, or *Simple* mechanical properties or with *Extension-Shearing* and/or *Bending-Twisting* couplings. All designs can be achieved without the need for deposition with off-axis alignment. However, this

results is a marked reduction in the available design space for NCF laminates, in comparison to their UD counterparts; differences of up to an order of magnitude have been revealed in most ply number groupings.

Lamination parameter design spaces, containing point clouds representing individual laminate designs, have been used to illustrate the severe constraint imposed by NCF architecture. The constraint of imposing an angle ply on the upper surface of the laminate gives rise to two distinctly separate NCF designs.

For tapered solutions, in which a continuous outer layer is assumed, these two sets of designs are non-compatible. Nevertheless, a two-layer termination algorithm has been successfully employed to develop permissible tapered designs for new NCF laminates in which consistent mechanical *Extension-Shearing Bending-Twisting* coupling characteristics and immunity to thermal warping distortion are preserved.

Acknowledgements

The Newton Research Collaboration Programme (NRCP1516/4/50) and Conselho Nacional de Desenvolvimento Científico e Tecnológico (CNPq 309545/2015-3 and 574004/2008-4) are gratefully acknowledged for supporting this research.

References

- [1] K. He, S.V. Hoa and R. Ganesan “The study of tapered laminated composite structures: A review”. *Composites Science and Technology*, Vol. 60, No. 14, pp. 2643-2657, 2000.

- [2] P. Dhurvey and N. D. Mittal “Review on various studies of composite laminates with ply drop-off”. *Journal of Engineering and Applied Sciences*, Vol. 8, No. 8, pp. 595-605, 2013.
- [3] A. Fletcher, R. Butler and T.J. Dodwell “Anti-symmetric laminates for improved consolidation and reduced warp of tapered C-sections”. *Advanced Manufacturing: Polymer & Composite Science*, Vol. 1, No. 2, pp. 105-111, 2015.
- [4] C. B. York “A Two-Ply Termination Strategy For Mechanically Coupled Tapered Laminates”. *Proceedings of the 20th International Conference on Composite Materials ICCM-20, Copenhagen, Denmark*, July 19-24, 2015.
- [5] F.-X. Irisarri, A. Lasseigne and F.-H. Leroy and R. Le Riche, “Optimal design of laminated composite structures with ply drops using stacking sequence tables”. *Composite Structures*, Vol. 107, pp. 559-569, 2014.
- [6] S. Tsai “Weight and cost reduction by using unbalanced and unsymmetric laminates”. *Proc. 18th International Conference on Composite Materials*, Jeju, Korea, 2011.
- [7] M.H. Shamsudin and C.B. York “On Mechanically Coupled Tapered Laminates with Balanced Plain Weave and Non-Crimp Fabrics”. *Proceedings of the 20th International Conference on Composite Materials ICCM-20, Copenhagen, Denmark*, July 19-24, 2015.
- [8] C.B. York “On tapered warp-free laminates with single-ply terminations”. *Composites Part A: Applied Science and Manufacturing*, Vol. 72, pp. 127-138, 2015.
- [9] C.B. York “Characterization of non-symmetric forms of fully orthotropic laminates, *AIAA J. Aircraft*, Vol. 46, pp. 1114-1125, 2009.

- [10] C.B. York “On Extension-Shearing coupled laminates”. *Composite Structures*, Vol. 120, pp. 472-448, 2015.
- [11] C.B. York “On Bending-Twisting coupled laminates”. *Composite Structures*, Vol. 160, pp. 887-900, 2017.
- [12] C.B. York and S.F.M. Almeida “On Extension-Shearing Bending-Twisting coupled laminates”. *Composite Structures*. Accepted for publication.
- [13] Engineering Sciences Data Unit “Stiffnesses of laminated plates”. ESDU Item No. 94003, IHS, 1994.
- [14] C. B. York “Unified approach to the characterization of coupled composite laminates: benchmark configurations and special cases”. *Journal of Aerospace Engineering*, Vol. 23, pp. 219-242, 2010.
- [15] C.B. York and S.F.M. Almeida “Effect of bending-twisting coupling on the compression and shear buckling strength of infinitely long plates”. *Composite Structures*, Submitted for possible publication.
- [16] S.W. Tsai and H.T. Hahn “*Introduction to composite materials*”. Technomic Publishing Co. Inc., Lancaster, 1980.
- [17] M. Miki “Material Design of Composite Laminates with Required In-Plane Elastic Properties”. *Proceedings of the 9th International Conference on Composite Materials, 1725-1731, Montreal, Canada, 1982*.
- [18] H. Fukunaga, and G.N. Vanderplaats “Stiffness optimization of orthotropic laminated composites using lamination parameters”. *AIAA Journal*, Vol. 29, pp. 641-646, 1991.

- [19] A. Vincenti, G. Verchery and P. Vannucci “Anisotropy and symmetry for elastic properties of laminates reinforced by balanced fabrics”. *Composites Part A: Applied Science and Manufacturing*, Vol. 32, pp. 1525–1532. 2001.
- [20] M.H. Shamsudin and C.B. York “Mechanically coupled laminates with balanced plain weave”. *Composite Structures*, Vol. 107, pp. 416-428. 2014.
- [21] D. Baker “Response of Damaged and Undamaged Tailored Extension-Shear-Coupled Composite Panels”. *J. Aircraft*, Vol. 43, pp. 517-527, 2006.

Tables

Table 1. Number of Non-crimp fabric (NCF) vs Uni-directional (UD) laminate solutions for each layer(ply) number grouping, $n_{\text{NCF}}(n_{\text{UD}})$, for fully uncoupled or *Simple* laminates, *Bending-Twisting* or *B-T* coupled laminates, *Extension-Shearing* or *E-S* coupled laminate and *Extension-Shearing Bending-Twisting* or *E-S;B-T* coupled laminates.

$n_{\text{NCF}}(n_{\text{UD}})$	<i>Simple</i>	<u><i>B-T</i></u>	<u><i>E-S</i></u>	<u><i>E-S;B-T</i></u>
4(8)	1(1)	6(12)	—	11(35)
5(10)	1(4)	—(42)	—	1(149)
6(12)	6(22)	54(203)	—	124(675)
7(14)	7(74)	19(980)	—	66(3,551)
8(16)	39(260)	607(5,927)	—	1,625(20,363)

Table 2. Number of Non-crimp fabric (NCF) laminate solutions, with equivalent number of Uni-directional (UD) plies for each layer(ply) number grouping, $n_{\text{NCF}}(n_{\text{UD}})$, for fully uncoupled or *Simple* laminates, *Bending-Twisting* or *B-T* coupled laminates, *Extension-Shearing* or *E-S* coupled laminate and *Extension-Shearing Bending-Twisting* or *E-S;B-T* coupled laminates. All NCF laminate solutions possess a \pm/\bigcirc upper surface layer.

$n_{\text{NCF}}(n_{\text{UD}})$	<i>Simple</i>	<u><i>B-T</i></u>	<u><i>E-S</i></u>	<u><i>E-S;B-T</i></u>
4(8)	—	2	—	7
5(10)	—	—	—	1
6(12)	—	20	—	72
7(14)	3	15	—	28
8(16)	5	242	—	890
9(18)	17	363	—	739
10(20)	56	3,561	—	13,760
11(22)	160	7,967	—	21,827
12(24)	726	69,805	5	250,598

Table 3. Number of Non-crimp fabric (NCF) laminate solutions, with equivalent number of Uni-directional (UD) plies for each layer(ply) number grouping, $n_{\text{NCF}}(n_{\text{UD}})$, for fully uncoupled or *Simple* laminates, *Bending-Twisting* or *B-T* coupled laminates, *Extension-Shearing* or *E-S* coupled laminate and *Extension-Shearing Bending-Twisting* or *E-S;B-T* coupled laminates. All NCF laminate solutions possess a $\pm/\text{—}$ upper surface layer.

$n_{\text{NCF}}(n_{\text{UD}})$	<i>Simple</i>	<u><i>B-T</i></u>	<u><i>E-S</i></u>	<u><i>E-S;B-T</i></u>
4(8)	1	4	—	4
5(10)	1	—	—	—
6(12)	6	34	—	52
7(14)	4	4	—	38
8(16)	34	365	—	735
9(18)	28	362	—	724
10(20)	223	4,774	—	12,316
11(22)	282	8,895	—	20,697
12(24)	1,851	81,604	2	236,590

Table 4. Stacking sequences for each layer(ply) number grouping, $n_{NCF}(n_{UD})$, for laminate designs with Quasi-Homogeneous *Extension-Shearing* and *Bending-Twisting* or *E-S;B-T* coupling, where 0/45, 0/-45, 45/-45 and 0/90, become -45/0, 45/0, -45/45 and 90/0 by inverting, respectively. Lamination parameter co-ordinates are given for each stacking sequence, representing identical extensional stiffness ($\xi_{\Delta}^A, \xi_R^A, \xi_{\Delta c}^A$) and bending stiffness ($\xi_{\Delta}^D, \xi_R^D, \xi_{\Delta c}^D$).

$n_{NCF}(n_{UD})$	Stacking sequence	$(\xi_{\Delta}^A, \xi_R^A, \xi_{\Delta c}^A) = (\xi_{\Delta}^D, \xi_R^D, \xi_{\Delta c}^D)$
4(8)	<u>45/0/0/45/0/45/45/0</u>	(0.50,0.00,0.50)
7(14)	<u>45/-45/0/-45/-45/0/0/45/45/-45/-45/45/-45/0</u>	(0.29,-0.43,-0.14)
8(16)	<u>45/-45/0/45/0/45/45/-45/-45/45/45/0/45/0/-45/45</u>	(0.25,-0.50,0.25)
	<u>45/0/(-45/45)₂/45/0/0/45/(45/-45)₂/0/45</u>	(0.25,-0.50,0.25)
	<u>45/0/(0/45)₂/45/0/0/45/(45/0)₂/0/45</u>	(0.50,0.00,0.50)
	<u>45/0/-45/0/-45/45/(45/0)₂/0/-45/45/-45/45/0</u>	(0.38,-0.25,0.13)
	<u>45/0/(0/45)₂/(45/0)₂/(0/45)₂/45/0</u>	(0.50,0.00,0.50)
	<u>45/0/0/45/45/0/(0/45)₂/45/0/0/45/45/0</u>	(0.50,0.00,0.50)
	<u>(45/0)₂/(0/45)₄/(45/0)₂</u>	(0.50,0.00,0.50)
	<u>45/-45/(0/-45)₂/-45/0/(0/-45)₂/-45/0/-45/45/45/-45/(-45/0)₂</u>	(0.36,-0.27,-0.27)
11(22)	<u>(45/-45)₂/-45/0/0/-45/45/-45/0/45/-45/45/45/-45/(-45/45)₂/-45/0</u>	(0.18,-0.64,-0.09)
	<u>45/0/-45/0/-45/45/0/45/-45/45/45/0/(0/-45)₃/45/-45/45/0</u>	(0.36,-0.27,0.09)
	<u>45/0/-45/45/-45/0/0/45/-45/0/0/45/45/-45/0/45/45/-45/0/-45/45/0</u>	(0.36,-0.27,0.09)
	<u>(45/0)₂/0/-45/-45/0/45/0/-45/45/0/45/45/0/(0/45)₂/0/-45</u>	(0.45,-0.09,0.18)
	<u>45/0/(-45/0)₂/0/-45/-45/0/-45/45/0/-45/0/45/45/0/(0/-45)₂</u>	(0.45,-0.09,-0.18)
	<u>45/-45/(0/45)₂/-45/45/45/0/(45/-45)₃/(0/45)₃/45/-45</u>	(0.25,-0.50,0.25)
	<u>45/-45/(-45/0)₃/(45/-45)₃/0/-45/-45/45/(-45/0)₂/45/-45</u>	(0.25,-0.50,-0.25)
	<u>45/-45/0/45/45/-45/(0/45)₂/-45/45/45/0/(45/-45)₂/0/45/45/-45/0/45</u>	(0.25,-0.50,0.25)

Table 5. Number of *tapered* solutions for *Extension-Shearing* and *Bending-Twisting* or *E-S;B-T* coupled warp-free laminates corresponding to n_{NCF} , with NCF layers and equivalent number, n_{UD} , with UD plies, with \pm/O surface layer for (a) even and (b) odd layer groupings. Column (2) is repeated from Table 2. Column (3) is the number of laminates from column (2) after applying $n_{\text{NCF}}-2$ top-down termination scheme. Column (4) is the number of laminates from column (3) matching laminates with $n_{\text{NCF}}+2$ after applying the *continuous* bottom-up termination scheme.

(a)			
(1)	(2)	(3)	(4)
$n_{\text{NCF}}(n_{\text{UD}})$			
12(24)	250,598	200,238 (250,598)	:
10(20)	13,760	11,058 (13,760)	:
8(16)	890	739 (890)	647
6(12)	72	66 (72)	66
4(8)	7	- (7)	7
(b)			
(1)	(2)	(3)	(4)
$n_{\text{NCF}}(n_{\text{UD}})$			
11(22)	21,827	10,403 (21,827)	:
9(18)	739	303 (739)	109
7(14)	28	7 (28)	7
5(10)	1	- (1)	1

Table 6. Number of *tapered* solutions for *Extension-Shearing* and *Bending-Twisting* or *E-S;B-T* coupled warp-free laminates corresponding to n_{NCF} , with NCF layers and equivalent number, n_{UD} , with UD layers, with \pm/\pm surface layer for (a) even and (b) odd layer groupings. Column (2) is repeated from Table 3. Column (3) is the number of laminates from column (2) after applying $n_{\text{NCF}}-2$ top-down termination scheme. Column (4) is the number of laminates from column (3) matching laminates with $n_{\text{NCF}}+2$ after applying the *continuous* bottom-up termination scheme.

(a)			
(1)	(2)	(3)	(4)
$n_{\text{NCF}}(n_{\text{UD}})$			
12(24)	236,590	184,802 (236,590)	:
10(20)	12,316	9,456 (12,316)	:
8(16)	735	606 (735)	480
6(12)	52	44 (52)	44
4(8)	4	- (4)	4
(b)			
(1)	(2)	(3)	(4)
$n_{\text{NCF}}(n_{\text{UD}})$			
11(22)	20,697	9,956 (20,697)	:
9(18)	724	384 (724)	384
7(14)	38	- (38)	38
5(10)	-	- (-)	-

Figures

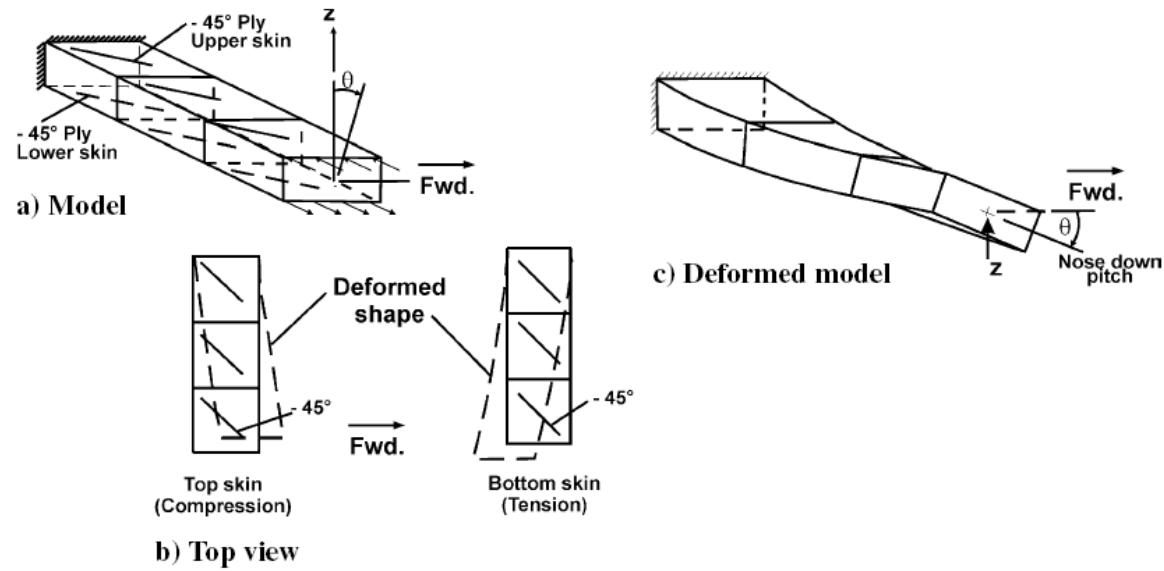


Figure 1 – Cantilever box-beam model (*after Ref. 21*) showing (a) general configuration, uniform stresses due to bending (force resultant acting through shear centre) and relative ply orientations for top and bottom skin; (b) relative deformations (exaggerated) between top and bottom skin and; (c) *Bending-Twisting* coupling deformation (exaggerated) arising from unbalanced laminate skins.

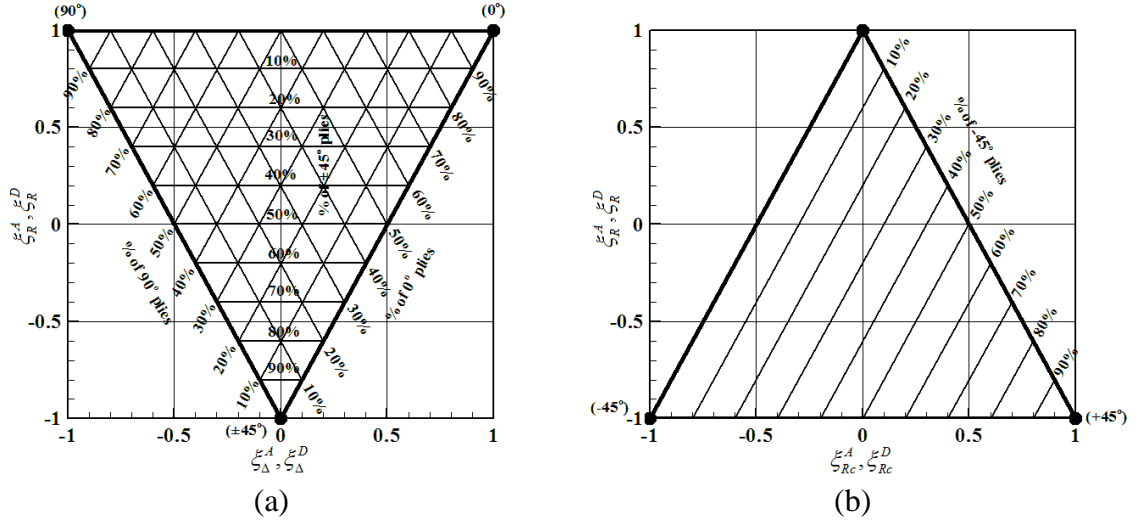
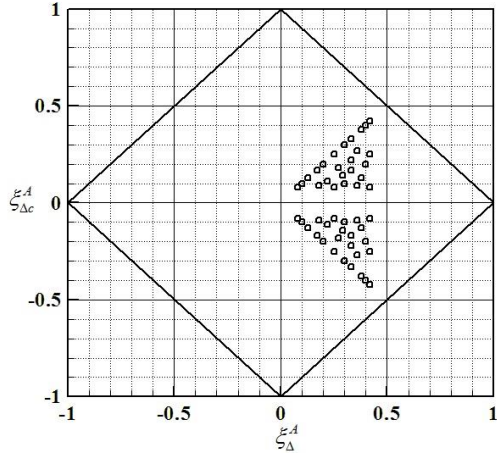
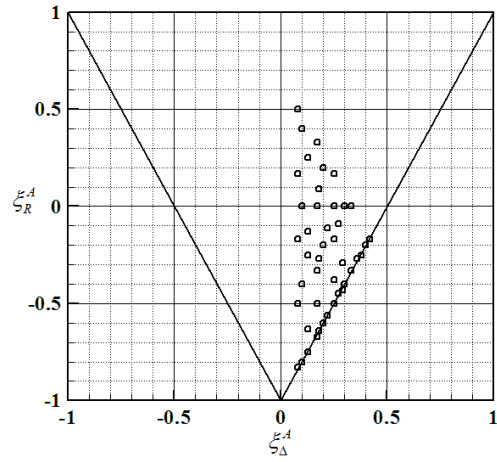


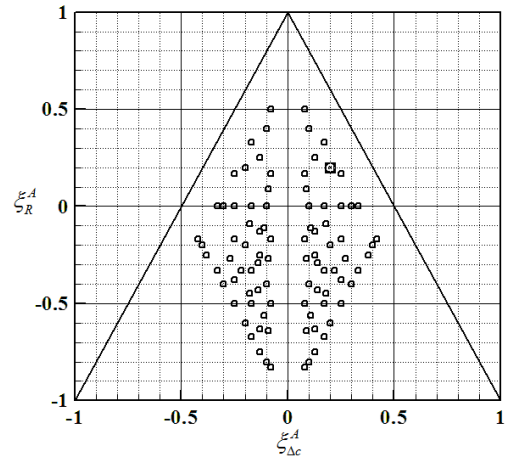
Figure 2 – Lamination parameter design space with ply percentages mapping for: (a) orthotropic stiffness (ξ_Δ^A, ξ_R^A), indicating the sub-region used in practical design and; (b) anisotropic stiffness ($\xi_{\Delta c}^A$) relating to differing angle-ply percentages. Note that ply percentages are related to bending stiffness for Quasi-Homogeneous laminates, where $\xi_\Delta^A = \xi_\Delta^D$, $\xi_R^A = \xi_R^D$ and $\xi_{\Delta c}^A = \xi_{\Delta c}^D$.



(a)

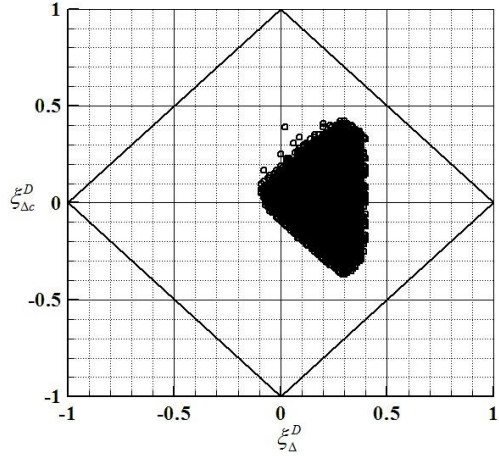


(b)

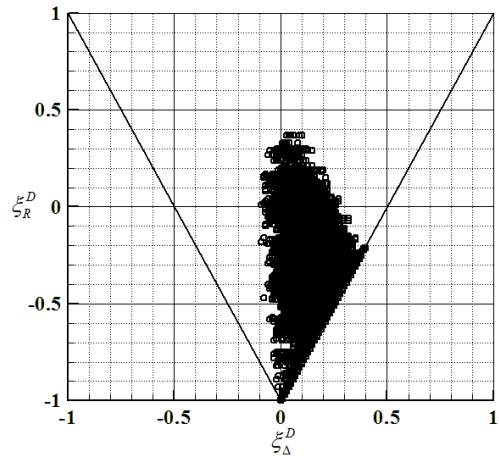


(c)

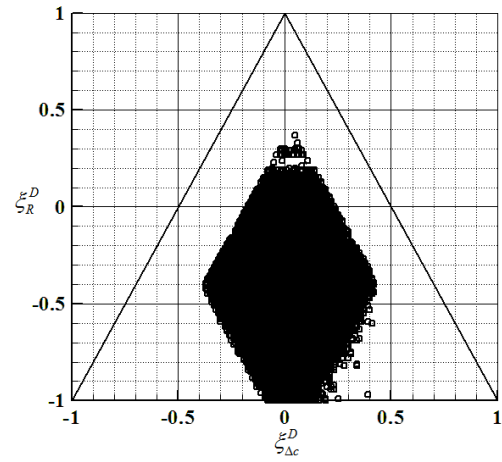
Figure 3 – Lamination parameter design space for: (a) – (c) extensional stiffness in *Extension-Shearing* and *Bending-Twisting* coupled NCF laminates with $4 \leq n_{\text{NCF}} \leq 12$ with \pm/\mp upper surface layer.



(a)



(b)



(c)

Figure 4 – Lamination parameter design space for: (a) – (c) bending stiffness in *Extension-Shearing* and *Bending-Twisting* coupled NCF laminates with $4 \leq n_{\text{NCF}} \leq 12$ with \pm/\pm upper surface layer.

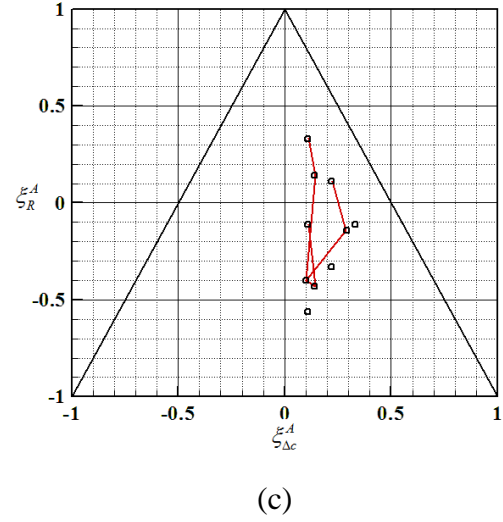
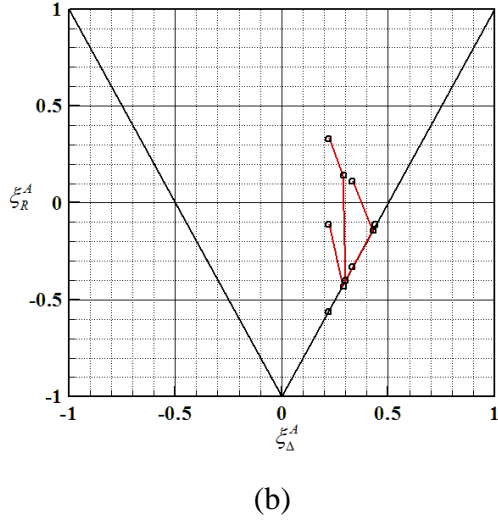
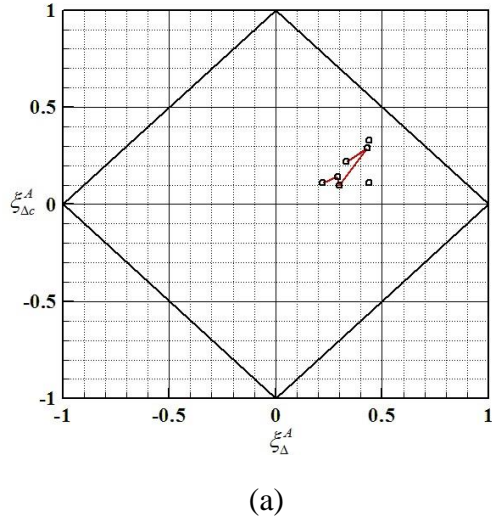


Figure 5 – Lamination parameter design space for: (a) – (c) extensional stiffness in Tapered *Extension-Shearing* and *Bending-Twisting* coupled NCF laminates with $n_{\text{NCF}} = 9 - 7 - 5$, with $\pm/\underline{\text{Q}}$ upper surface layer. All designs begin from the unique 5 layer NCF with coordinate $(\xi_{\Delta}^A, \xi_R^A, \xi_{\Delta c}^A) = (0.30, -0.40, 0.10)$.

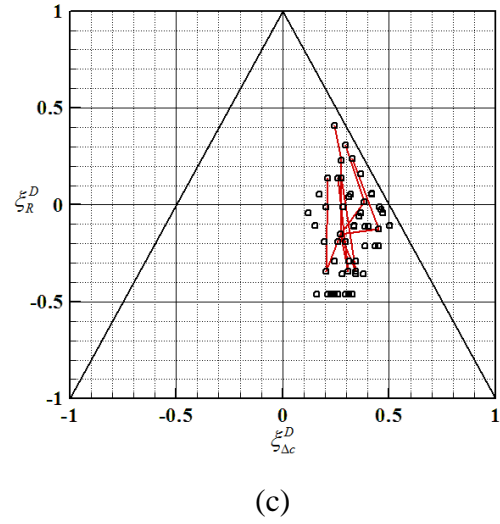
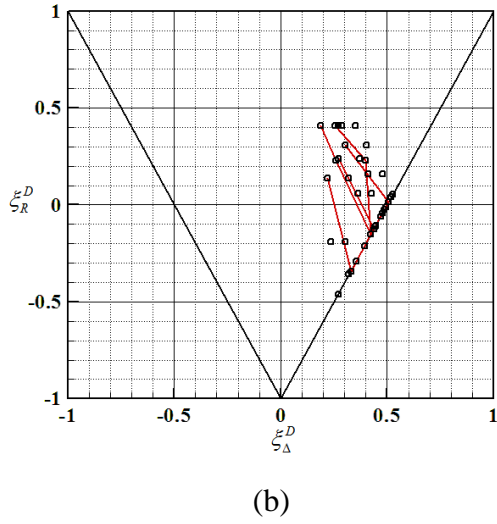
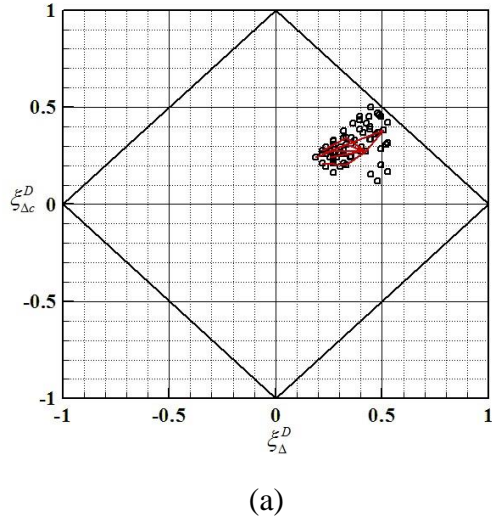


Figure 6 – Lamination parameter design space for: (a) – (c) bending stiffness in Tapered *Extension-Shearing* and *Bending-Twisting* coupled NCF laminates with $n_{\text{NCF}} = 9 - 7 - 5$, with $\pm/\underline{\text{O}}$ upper surface layer. All designs begin from the unique 5 layer NCF with coordinate $(\xi_{\Delta}^D, \xi_R^D, \xi_{\Delta c}^D) = (0.42, -0.15, 0.27)$.

Electronic Appendix

This electronic appendix to the main article on *Tapered laminate designs for new Non-Crimp Fabric architectures* contains:

A figure describing the 4 classes of mechanically coupled laminate investigated

- In-plane thermal contraction responses (Figure)

Stacking sequence listings

- *Extension-Shearing* coupled laminates (Table A1) with $n_{\text{NCF}}(n_{\text{UD}}) = 12(24)$ layers;
- Tapered examples (Tables A2), the first of which corresponds to Figs 5 and 6 of the main manuscript.

Design space comparisons

- third angle orthographic projections (Figs A3 – A7) for 2- and 3-dimensional design spaces, corresponding to extensional $(\xi_{\Delta}^A, \xi_R^A, \xi_{\Delta c}^A)$ and bending $(\xi_{\Delta}^D, \xi_R^D, \xi_{\Delta c}^D)$ stiffness lamination parameters, when standard ply angles 0° , $\pm 45^\circ$ and 90° are adopted.

Mechanically Coupled Laminates

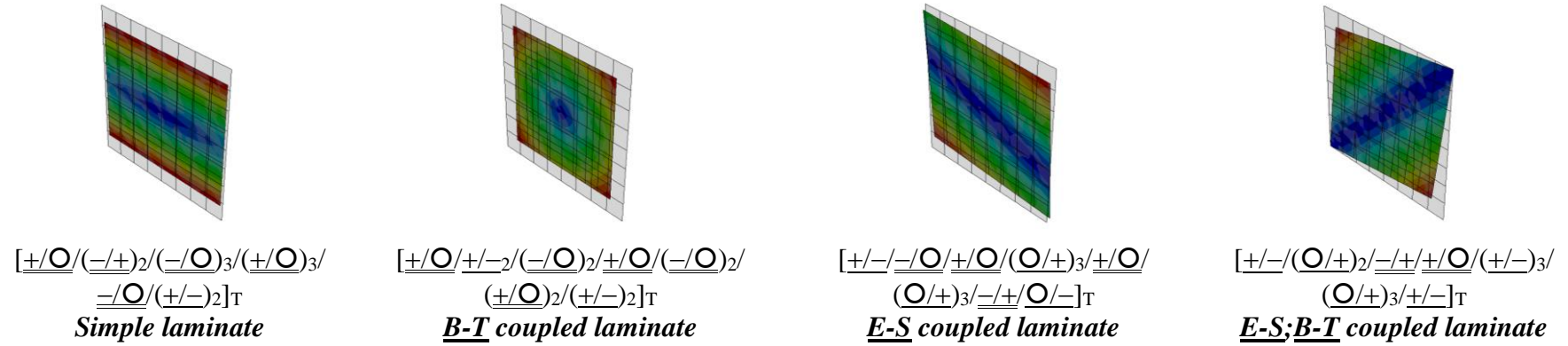


Figure A1 – In-plane thermal contraction responses (not to scale) resulting from a typical high temperature curing process. All examples shown are square, initially flat, composite laminates. The example stacking sequences are 24-ply laminates and are given in symbolic form, where symbols +, –, O and ● are used in place of standard ply orientations $\pm 45^\circ$, 0° and 90° , respectively. The underlining highlights the NCF ply pairings.

Stacking sequence listings

Extension-Shearing coupled laminates were found only in the highest layer (ply) number grouping investigated, i.e. $n_{\text{NCF}}(n_{\text{UD}}) = 12$ (24). The small number of stacking sequences for this class of laminate are listed in Table A1, together with the lamination parameter coordinates.

Table A1. Stacking sequences for $n_{\text{NCF}}(n_{\text{UD}}) = 12(24)$ layer laminate designs with *Extension-Shearing* or *E-S* coupling, where 0/45, 0/-45, 45/-45 and 0/90, become -45/0, 45/0, -45/45 and 90/0 by inverting, respectively.

Stacking sequence	$(\xi_{\Delta}^A, \xi_R^A, \xi_{\Delta c}^A), (\xi_{\Delta}^D, \xi_R^D)$
<u>45/-45/-45/0/0/45/45/0/0/45/45/0/(0/45)₄/-45/45/0/-45</u>	(0.42,-0.17,0.25), (0.30,-0.41)
<u>45/-45/-45/0/45/0/(0/45)₃/45/0/(0/45)₃/-45/45/0/-45</u>	:
<u>45/0/-45/45/(-45/0)₃/0/-45/(-45/0)₃/0/-45/0/45/45/-45</u>	(0.42,-0.17,-0.25), (0.30,-0.41)
<u>45/0/-45/45/(-45/0)₄/0/-45/-45/0/0/-45/-45/0/0/45/45/-45</u>	:
<u>45/0/0/-45/0/-45/45/-45/(-45/0)₄/0/-45/45/-45/-45/0/45/0</u>	(0.42,-0.17,-0.25), (0.45,-0.09)
<u>45/0/0/-45/-45/0/45/-45/0/-45/-45/0/0/-45/-45/0/45/-45/0/45/0</u>	:
<u>45/0/-45/0/0/-45/45/-45/(0/-45)₂/(-45/0)₃/45/-45/-45/0/45/0</u>	:

Table A2(a) contains stacking sequence information for all compatible designs for $n_{\text{NCF}} = 9 - 7 - 5$, including lamination parameter coordinates, illustrated in Figs 5 and 6 of the main manuscript. Table A2(a) designs are dominated by cross-ply terminations, whilst alternative designs listed in Table A2(b) are dominated by angle-ply terminations. All stacking sequences are non-symmetric, yet retain *Extension-Shearing Bending-Twisting* coupling and warp free characteristic throughout. Layer terminations are indicated in bold, to clearly illustrate that these are neither necessarily symmetrically disposed about the laminate mid-plane, nor restrained to a central ply block. Stacking sequences that share the same lamination parameter coordinates are identical, but have multiple layer termination possibilities due to the presence of repeated layers.

Table A2. Example *tapered* solutions for *Extension-Shearing* and *Bending-Twisting* coupled laminates with lamination parameter coordinates for: (a) cross-ply and (b) angle-ply dominated layer terminations. The first three stacking sequences represent one of the seven ($n_{\text{NCF}} = 9 - 7 - 5$) strings illustrated in Figs 5 and 6; the remainder are alternative solutions for $n_{\text{NCF}} = 9$. Layer terminations are indicated in bold.

(a)

$n_{\text{NCF}}(n_{\text{UD}})$	Stacking sequence	$(\xi_{\Delta}^A, \xi_R^A, \xi_{\Delta c}^A), (\xi_{\Delta}^D, \xi_R^D, \xi_{\Delta c}^D)$
5(10)	<u>45/0/-45/0/45/0/45/-45/45/0</u>	(0.30,-0.40,0.10), (0.42,-0.15,0.27)
7(14)	<u>45/0/90/0/-45/0/45/0/45/-45/0/90/45/0</u>	(0.29,0.14,0.14), (0.26,0.23,0.27)
9(18)	<u>45/0/90/0/90/0/-45/0/45/0/45/-45/0/90/0/90/45/0</u>	(0.22,0.33,0.11), (0.19,0.41,0.24)
	<u>45/0/90/0/90/0/-45/0/45/0/45/-45/0/90/0/90/45/0</u>	:
	<u>45/0/90/0/90/0/-45/0/45/0/45/-45/0/90/0/90/45/0</u>	:
	<u>45/0/90/0/90/0/-45/0/45/0/45/-45/0/90/0/90/45/0</u>	:
	<u>45/0/90/0/-45/45/-45/0/45/0/45/-45/45/-45/0/90/45/0</u>	(0.22,-0.11,0.11), (0.22,0.14,0.21)
	<u>45/0/90/0/-45/45/-45/0/45/0/45/-45/45/-45/0/90/45/0</u>	:
	<u>45/0/90/0/45/-45/-45/0/45/0/-45/45/45/-45/0/90/45/0</u>	(0.22,-0.11,0.11), (0.22,0.14,0.26)
	<u>45/0/90/0/45/0/-45/0/45/0/45/-45/0/45/0/90/45/0</u>	(0.33,0.11,0.22), (0.27,0.24,0.33)
	<u>45/0/90/0/0/45/-45/0/45/0/45/-45/45/0/0/90/45/0</u>	(0.33,0.11,0.22), (0.30,0.31,0.29)
	<u>45/0/90/0/45/-45/-45/0/45/0/45/-45/-45/45/0/90/45/0</u>	(0.22,-0.11,0.11), (0.22,0.14,0.28)
	<u>45/0/90/0/0/90/-45/0/45/0/45/-45/90/0/0/90/45/0</u>	(0.22,0.33,0.11), (0.25,0.41,0.24)
	<u>45/0/0/90/90/0/-45/0/45/0/45/-45/90/0/0/90/45/0</u>	:
	<u>45/0/-45/45/90/0/-45/0/45/0/45/-45/0/90/45/-45/45/0</u>	(0.22,-0.11,0.11), (0.24,-0.19,0.19)
	<u>45/0/45/0/90/0/-45/0/45/0/45/-45/0/90/0/45/45/0</u>	(0.33,0.11,0.22), (0.36,0.06,0.42)
	<u>45/0/0/45/90/0/-45/0/45/0/45/-45/0/90/45/0/45/0</u>	(0.33,0.11,0.22), (0.41,0.16,0.37)
	<u>45/0/45/-45/90/0/-45/0/45/0/45/-45/0/90/-45/45/45/0</u>	(0.22,-0.11,0.11), (0.24,-0.19,0.29)
	<u>45/0/90/0/0/90/-45/0/45/0/45/-45/0/90/90/0/45/0</u>	(0.22,0.33,0.11), (0.27,0.41,0.24)
	<u>45/0/0/90/90/0/-45/0/45/0/45/-45/0/90/90/0/45/0</u>	:

(b)

$n_{NCF}(n_{UD})$	Stacking sequence	$(\xi_{\Delta}^A, \xi_R^A, \xi_{\Delta c}^A), (\xi_{\Delta}^D, \xi_R^D, \xi_{\Delta c}^D)$
5(10)	<u>45/0/-45/0/45/0/45/-45/45/0</u>	(0.30,-0.40,0.10), (0.42,-0.15,0.27)
7(14)	<u>45/0/-45/45/-45/0/45/0/45/-45/45/-45/45/0</u>	(0.29,-0.43,0.14), (0.33,-0.34,0.20)
	<u>45/0/-45/45/-45/0/45/0/45/-45/45/-45/45/0</u>	:
9(18)	<u>45/0/90/0/-45/45/-45/0/45/0/45/-45/45/-45/0/90/45/0</u>	(0.22,-0.11,0.11), (0.22,0.14,0.21)
	<u>45/0/-45/45/90/0/-45/0/45/0/45/-45/0/90/45/-45/45/0</u>	(0.22,-0.11,0.11), (0.24,-0.19,0.19)
	<u>45/0/-45/45/-45/45/-45/0/45/0/45/-45/45/-45/45/-45/45/0</u>	(0.22,-0.56,0.11), (0.27,-0.46,0.16)
	<u>45/0/-45/45/-45/45/-45/0/45/0/45/-45/45/-45/45/-45/45/0</u>	:
	<u>45/0/-45/45/-45/45/-45/0/45/0/45/-45/45/-45/45/-45/45/0</u>	:
	<u>45/0/-45/45/-45/45/-45/0/45/0/45/-45/45/-45/45/-45/45/0</u>	:
	<u>45/0/-45/45/-45/45/-45/0/45/0/45/-45/45/-45/45/-45/45/0</u>	:
	<u>45/0/-45/45/-45/45/-45/0/45/0/45/-45/45/-45/45/-45/45/0</u>	:
	<u>45/0/-45/45/45/-45/-45/0/45/0/45/-45/45/45/-45/45/-45/45/0</u>	(0.22,-0.56,0.11), (0.27,-0.46,0.21)
	<u>45/0/45/-45/-45/45/-45/0/45/0/45/-45/45/45/-45/45/-45/45/0</u>	(0.22,-0.56,0.11), (0.27,-0.46,0.23)
	<u>45/0/-45/45/45/0/-45/0/45/0/45/-45/0/45/45/-45/45/0</u>	(0.33,-0.33,0.22), (0.32,-0.36,0.28)
	<u>45/0/-45/45/0/45/-45/0/45/0/45/-45/45/0/45/-45/45/0</u>	(0.33,-0.33,0.22), (0.35,-0.29,0.25)
	<u>45/0/-45/45/45/-45/-45/0/45/0/45/-45/45/45/-45/45/0</u>	(0.22,-0.56,0.11), (0.27,-0.46,0.23)
	<u>45/0/45/-45/-45/45/-45/0/45/0/45/-45/45/45/-45/45/0</u>	(0.22,-0.56,0.11), (0.27,-0.46,0.24)
	<u>45/0/-45/45/0/90/-45/0/45/0/45/-45/90/0/45/-45/45/0</u>	(0.22,-0.11,0.11), (0.30,-0.19,0.19)
	<u>45/0/45/0/-45/45/-45/0/45/0/45/-45/45/-45/0/45/45/0</u>	(0.33,-0.33,0.22), (0.40,-0.21,0.39)
	<u>45/0/0/45/-45/45/-45/0/45/0/45/-45/45/-45/45/0/45/0</u>	(0.33,-0.33,0.22), (0.44,-0.11,0.34)
	<u>45/0/-45/45/45/-45/-45/0/45/0/45/-45/45/-45/45/45/0</u>	(0.22,-0.56,0.11), (0.27,-0.46,0.24)
	<u>45/0/45/-45/-45/45/-45/0/45/0/45/-45/45/-45/45/45/0</u>	(0.22,-0.56,0.11), (0.27,-0.46,0.26)
	<u>45/0/0/90/-45/45/-45/0/45/0/45/-45/45/-45/90/0/45/0</u>	(0.22,-0.11,0.11), (0.32,0.14,0.21)

Design space comparisons

The 2-dimensional projections for extensional and bending stiffness are illustrated in Figs A2 and A3 for *Simple* laminates with \pm/\pm and \pm/O upper surface layers, respectively. The point clouds of lamination parameter coordinates are significantly influenced by the outer surface layer architecture. Of the eight layer combinations, 0° plies are present in six. By contrast, only two layer combinations contain 90° plies, hence there is a design freedom constraint which introduces a bias in the results towards the 0° ply dominated region of the design space. This bias is strong in designs with \pm/O upper surface layers, which need to be balanced by additional 0° plies in order to eliminate *Extension-Bending* coupling. It is not diminished by the introduction of layers containing 90° plies, since these are paired with 0° plies. However, this biasing is substantially reduced in designs with \pm/\pm upper surface layers, which instead need to be balanced by additional angle ply layers to eliminate *Extension-Twisting* (and *Shearing-Bending*) coupling.

The 2- and 3-dimensional orthographic projections for extensional and bending stiffness are illustrated in Figs A4 and A5 for *Bending-Twisting* (*B-T*) coupled laminates. These results represent solutions with a \pm/\pm and \pm/O upper surface layers, respectively. The 3-dimensional orthographic projections for bending stiffness reveal that *Bending-Twisting* coupling, i.e. $\xi_{\Delta c}^D$, is generally higher in laminates with \pm/O upper surface layers.

The 3-dimensional point cloud of lamination parameters for *Extension-Shearing* *Bending-Twisting* or *E-S;B-T* coupled laminates, with \pm/O upper surface layers, are illustrated in Figs A6 and A7.

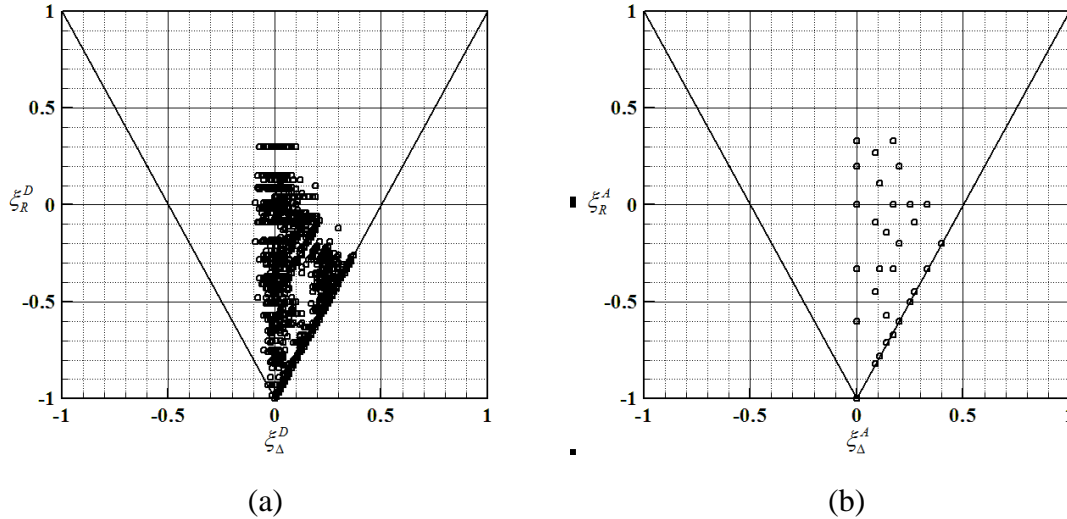


Figure A2 – Lamination parameter design space for: (a) bending and; (b) extensional stiffness in *Simple* NCF laminates with $4 \leq n_{\text{NCF}} \leq 12$ with \pm/\pm upper surface layer.

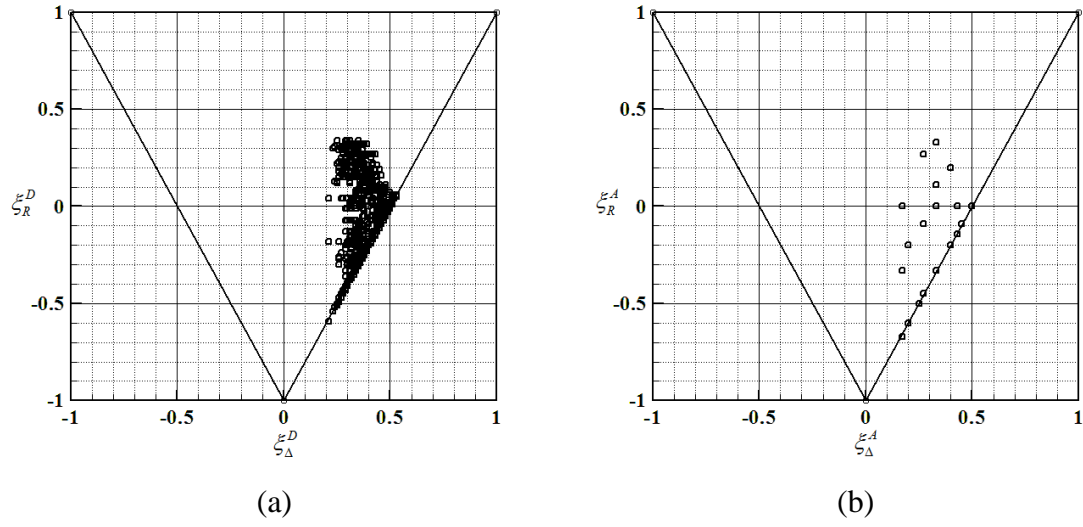
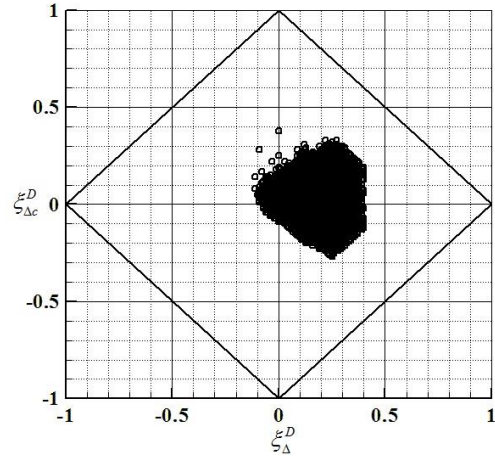
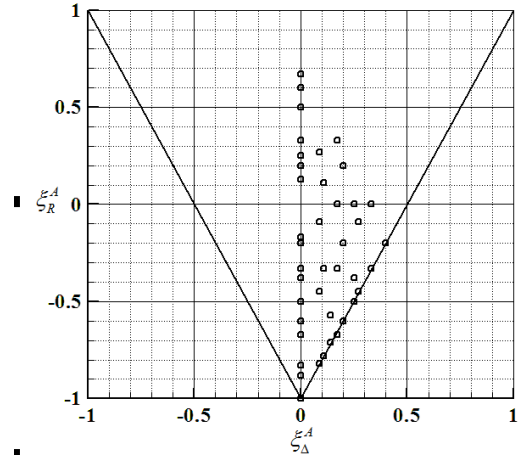


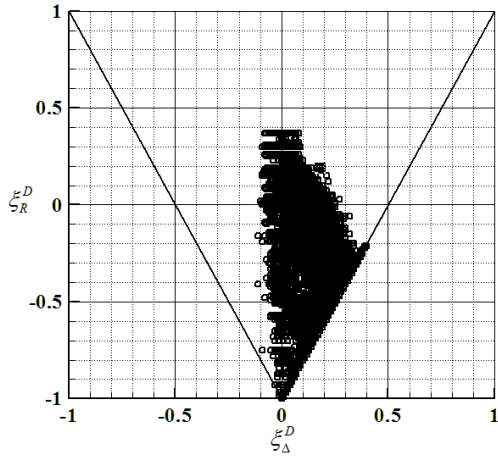
Figure A3 – Lamination parameter design space for: (a) bending and; (b) extensional stiffness in *Simple* NCF laminates with $4 \leq n_{\text{NCF}} \leq 12$ with $\underline{+/\underline{\bigcirc}}$ upper surface layer.



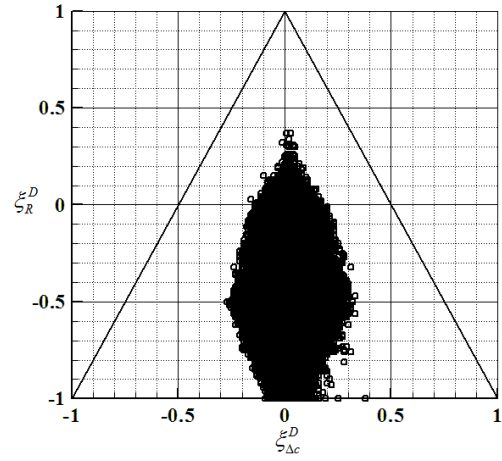
(a)



(d)

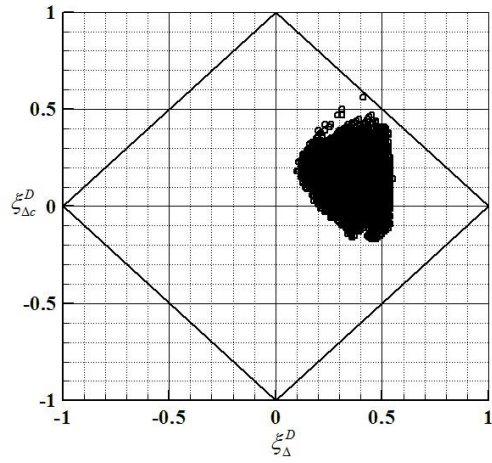


(b)

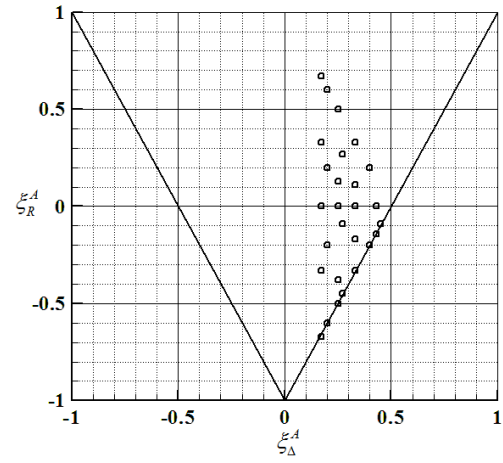


(c)

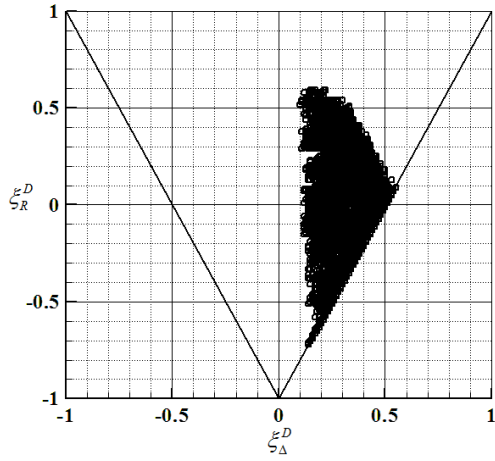
Figure A4 – Lamination parameter design space for: (a) – (c) bending stiffness and; (d) extensional stiffness in *Bending-Twisting* coupled NCF laminates with $4 \leq n_{\text{NCF}} \leq 12$ with \pm/\pm upper surface layer.



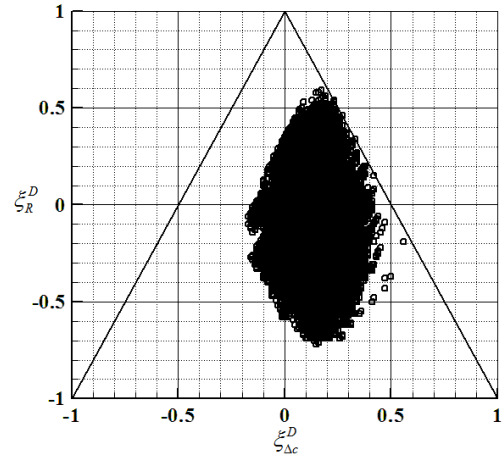
(a)



(d)



(b)



(c)

Figure A5 – Lamination parameter design space for: (a) – (c) bending stiffness and; (d) extensional stiffness in *Bending-Twisting* coupled NCF laminates with $4 \leq n_{\text{NCF}} \leq 12$ with $\pm/\underline{\text{O}}$ upper surface layer.

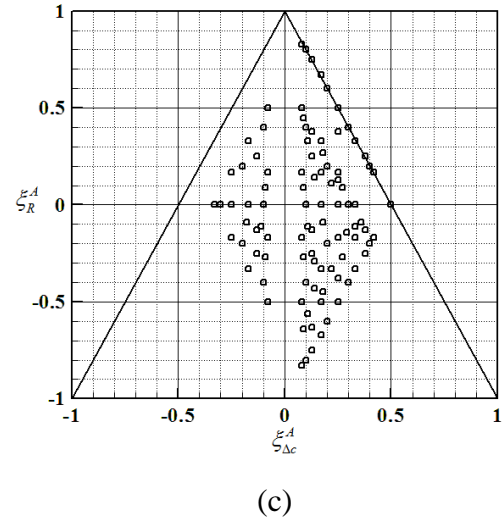
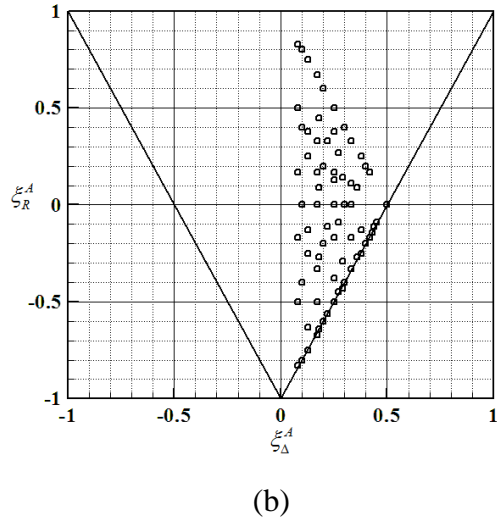
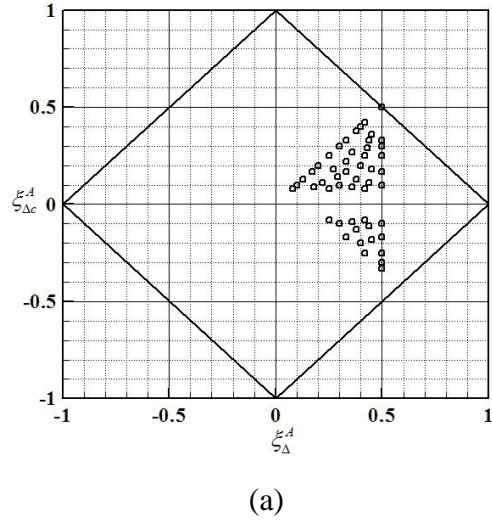
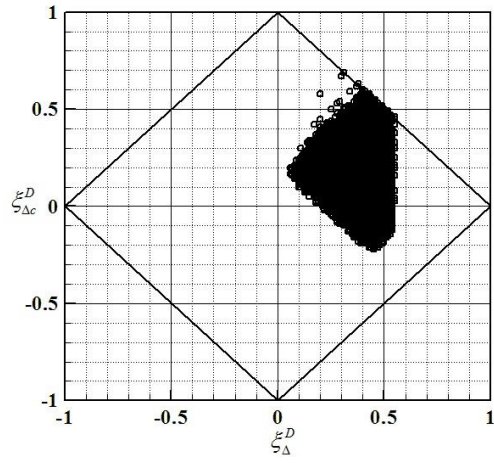
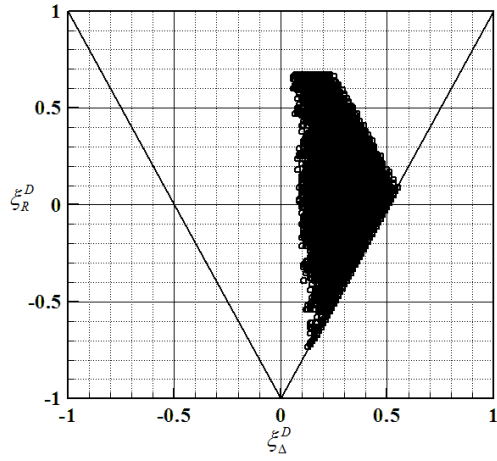


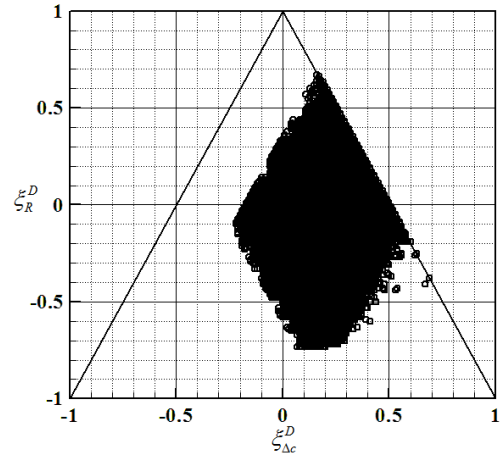
Figure A6 – Lamination parameter design space for: (a) – (c) extensional stiffness in *Extension-Shearing* and *Bending-Twisting* coupled NCF laminates with $4 \leq n_{\text{NCF}} \leq 12$ with $\pm/\underline{\text{O}}$ upper surface layer.



(a)



(b)



(c)

Figure A7 – Lamination parameter design space for: (a) – (c) bending stiffness in *Extension-Shearing Bending-Twisting* coupled NCF laminates with $4 \leq n_{\text{NCF}} \leq 12$ with \pm/O upper surface layer.